Astron. Astrophys. 325, 677–684 (1997)

ASTRONOMY
AND
ASTROPHYSICS

Inference of steady stellar wind $v(r)$ laws from optically thin emission lines

I. Idealised analysis for the profile of a single line

J.C. Brown[1], **L.L. Richardson**[1], **J.P. Cassinelli**[2], **and R. Ignace**[1]

[1] Department of Physics and Astronomy, University of Glasgow, Glasgow, UK
[2] Department of Astronomy, University of Wisconsin-Madison, USA

Received 28 August 1996 / Accepted 21 November 1996

Abstract. The form of the profile $F_{\lambda_0}(\Delta\lambda)$ of an emission line from a steady spherical wind of velocity profile $v(r)$ is derived for the case when optical depths are small, when stellar occultation of the wind is neglected, and when $v(r)$ is highly supersonic. It is shown how the resulting integral equation for $v(r)$, given $F_{\lambda_0}(\Delta\lambda)$, can be inverted to yield $v(r)$ if the line emissivity function $j(r)$ is known.

Solutions are demonstrated for simulated data in the case of a recombination line ($j \propto n^2$) for various trial forms of $v(r)$. The solution is unique provided $\mathrm{d}v/\mathrm{d}r$ does not change sign anywhere and is remarkably stable against noise in the $F_{\lambda_0}(\Delta\lambda)$ data. The analysis is idealised in the sense that the stellar mass loss rate $\dot{M}$ and distance D are assumed known, the solution being then carried out in scaled dimensionless variables. The absolute r-scale of the solution for given $F_{\lambda_0}(\Delta\lambda)$ scales as $(\dot{M}/D)^2$. If this quantity is known the method also yields the stellar radius.

Key words: lines: profile – stars: mass loss – numerical methods

1. Introduction

Formation of emission line profiles from hot stellar winds has been extensively discussed – see e.g. reviews by Lamers et al. (1987) and Hamann (1981) (also Lamers and Cassinelli 1997). Most treatments of this problem to date, however, deal with it by the 'forward' approach – line profiles are predicted from parametric wind models – rather than by an inverse approach where wind structure is inferred from line profile data. As in all 'inverse' problems (Craig and Brown 1986), the two approaches are potentially equivalent, but inversion has the advantage of yielding direct insight into the information content carried by line profile data regarding source structure and hence on the uniqueness/uncertainty of models consistent with noisy data. Such information can be deduced by forward computation from a variety of wind models but is usually limited by the need to compute a large grid of models and by restrictive parametric representations. An inverse solution, especially if analytic, brings out clearly the relationship between data and model, though usually only at the expense of some simplifying assumptions. One example of a semi-inverse parametric treatment is that by Cannon (1974) who used Wolf-Rayet line profiles to estimate the structure of the wind velocity, temperature and density, based on approximate radiative transfer expressions.

In the present paper, we address the line profile formation problem in the simple case where the wind is tenuous enough to be optically thin, in both lines and continuum, outside some sharp 'photospheric' radius. We thus neglect radiative transfer in the line and line broadening due to electron scattering, (most relevant to dense winds such as WR stars), deferring to a subsequent paper discussion of how these factors can be incorporated. We also ignore the finite size of the stellar disk – occultation of wind material behind the star and absorption of stellar disk radiation by wind material in front of it. Whilst recognising that these simplifications need to be removed for treatment of dense stellar (such as WR) winds, and those (e.g. OB) winds where emission is concentrated near the stellar surface, the simplicity of the analytic results obtained shed much light on the fundamental wind $v(r)$ problem in general. Like Cannon (1974), and many others, our treatment is only for steady spherically symmetric structures and does not address wind inhomogeneities or the corresponding narrow features these superpose on the main broad profile from the smoothed WR wind structure (Robert 1994, Moffat and Robert 1992, Brown et al. 1995).

2. Emission line profile from an optically thin steady spherical wind

We consider a line of rest wavelength λ_0 formed in a wind of speed $v(r)$ at distance r from the stellar centre and of total

Send offprint requests to: J.C. Brown

'emissivity' $j(r)$ (Wm^{-3}) at r. We neglect the width of the line in the rest frame, assuming the wind speed $v(r) >>$ the thermal speed of the emitting ions in the region concerned. On a spherical shell of radius r and thickness $\mathrm{d}r$ small enough for $v(r)$ to be taken as constant, photons from points on an annulus at angle θ between the directions of this point and of the observer are seen at wavelength shift

$$\Delta\lambda = \frac{\lambda_0}{c} v(r) \cos\theta \ , \tag{1}$$

and, from the range $\mathrm{d}\theta$, have a spread

$$\mathrm{d}\lambda = \mathrm{d}(\Delta\lambda) = \frac{\lambda_0}{c} v(r) \sin\theta \mathrm{d}\theta \ , \tag{2}$$

the contribution to the line power from $\mathrm{d}\theta$, $\mathrm{d}r$ being $2\pi r^2 j(r) \sin\theta \mathrm{d}r\mathrm{d}\theta$. In the spectral line profile this contribution is contained entirely within the wavelength range $(-\lambda_0 v(r)/c, +\lambda_0 v(r)/c)$ since $\cos\theta \leq 1$ in Eq. (1). If the total wind line luminosity spectrum is $L_\lambda(\Delta\lambda)$ (W per unit λ) at wavelength shift $\Delta\lambda$, then the contribution $\mathrm{d}L_\lambda$ to L_λ from the shell $\mathrm{d}r$, $\mathrm{d}\theta$ is given by,

$$\mathrm{d}L_\lambda(\Delta\lambda)\mathrm{d}(\Delta\lambda) = 2\pi r^2 j(r) \sin\theta \mathrm{d}r\mathrm{d}\theta \ , \tag{3}$$

or, using Eq. (2),

$$\mathrm{d}L_\lambda(\Delta\lambda) = \begin{cases} \frac{2\pi r^2 j(r) c}{\lambda_0 v(r)} \mathrm{d}r & \text{if } \Delta\lambda/\lambda_0 \leq v/c \\ 0 & \text{if } \Delta\lambda/\lambda_0 > v/c \end{cases} \tag{4}$$

which is a flat (rectangular) profile. (Such a profile contribution arises also from any *geometrically thick* shell, r_1, r_2, over which $v(r) = v_1$ is constant, viz.

$$L_\lambda^{\mathrm{shell}}(\Delta\lambda) = \begin{cases} \frac{2\pi c}{\lambda_0 v_1} \int_{r_1}^{r_2} r^2 j(r) \mathrm{d}r & \text{if } \Delta\lambda \leq \frac{v_1 \lambda_0}{c} \\ 0 & \text{if } \Delta\lambda > \frac{v_1 \lambda_0}{c} \end{cases} \tag{5}$$

– a well known result.)

For a general $v(r)$ structure, the total wind profile is determined by integrating Eq. (4) over all r from the sharply defined radius $R(\lambda_0)$ inside which the line concerned is taken to have effectively infinite optical depth –

$$L_\lambda(\Delta\lambda) = \frac{2\pi c}{\lambda_0} \int_{R(\lambda_0)}^{\infty} \frac{r^2 j(r)}{v(r)} H\left(\frac{c}{v(r)} \frac{\Delta\lambda}{\lambda_0}\right) \mathrm{d}r \tag{6}$$

where the Heaviside step function $H(a)$(= 1 for $0 \leq a \leq 1$, = 0 for $a > 1$) defines condition (4), i.e. we are integrating over all visible r such that $v(r) \geq c\Delta\lambda/\lambda_0$.

The line profile can thus be thought as the sum of a set of rectangular contributions from each $\mathrm{d}r$, the total width of which depends on $v(r)$ and the height on $r^2 j(r)\mathrm{d}r/v(r)$. This is illustrated schematically in Fig. 1 for a wind of monotonic $v(r)$ where the r intervals are meant to be such as to give similar total power $j(r)r^2\mathrm{d}r$ from each shell, where $j(r)$ decreases with r (as will usually be the case). Derivation of $v(r)$ from $L_\lambda(\Delta\lambda)$ for known $j(r)$ by differentiation, discussed below, can then be thought of as deconstructing line profile Fig. 1(c) into Fig. 1(b) then successively subtracting contributions from 4,3,2. . . .

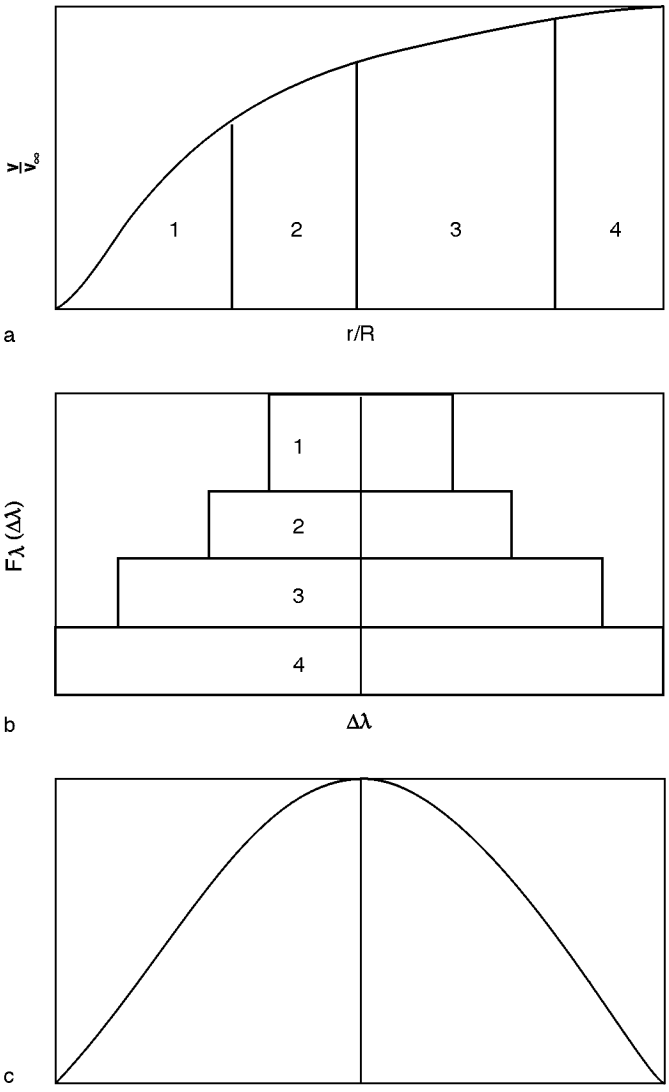

Fig. 1. Production of line profile (bottom panel) as a summation of contributions (middle panel) generated by different spatial segments of a wind with monotonic $v(r)$ (top panel)

An important feature to note about this process of line profile composition is that the summation is really a summation of contributions from successive intervals in v, rather than in r, though in Fig. 1 these correspond, since $v(r)$ was taken to be monotonic. In Fig. 2a we show schematically a non-monotonic $v(r)$, obtained by switching elements 2 and 3 in Fig. 1a and the corresponding element summation in Fig. 2b. The resulting line profile is identical to that in Fig. 1c. Consequently it is clear that *ambiguity exists* in the $v(r)$ needed to produce an optically thin line profile. Physically this is because, in a completely optically thin wind, different Δr elements can be interchanged (for specified $j(r)$) without changing the resulting emission line profile so long as the contributions from each Δv are not changed.

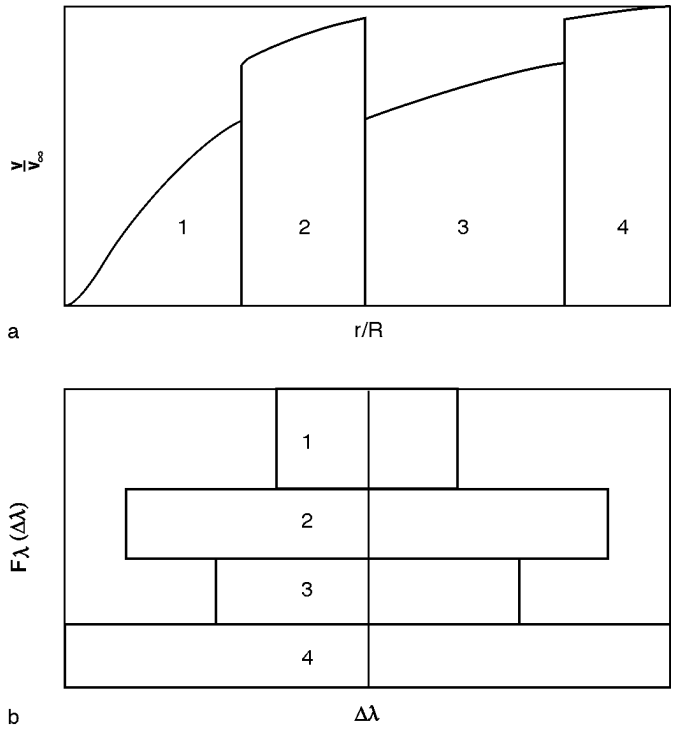

Fig. 2. Production of an identical line profile to that in Fig. 1c by summation of contributions (lower panel) generated by a non-monotonic wind profile $v(r)$ (top panel) obtained from a monotonic one by spatial interchange of elements

Detailed discussion of how such ambiguity can be resolved by use of multiple line profiles is deferred to a subsequent paper. For the present we focus solely on the solution obtained on the assumption of monotonic $v(r)$.

3. Analytic inversion for monotonic $v(r)$

If $v(r)$ is monotonic then Eq. (6) can be uniquely converted to an integral over v instead of r, namely (assuming $v' > 0$)

$$L_\lambda(\Delta\lambda) = \frac{2\pi c}{\lambda_0} \int_{v_{\min}(\Delta\lambda)}^{v_\infty} \frac{r^2(v) j(r(v))}{v \mathrm{d}v/\mathrm{d}r} \mathrm{d}v \ , \tag{7}$$

where

$$v_{\min}(\Delta\lambda) = \begin{cases} c\frac{\Delta\lambda}{\lambda_0} & c\frac{\Delta\lambda}{\lambda_0} \geq v_1 \\ v_1 & c\frac{\Delta\lambda}{\lambda_0} \leq v_1 \end{cases} \tag{8}$$

and v_1 is the (minimum) speed in the wind at the photosphere, $r = R$.

When $v_1 \neq 0$, the line profile has a flat central region out to a point $\Delta\lambda_1 = \lambda_0 v_1/c$. The presence of such a central flat region in an optically thin line profile from a wind of monotonic $v(r)$ *always* indicates a finite wind speed v_1 at the 'photosphere', $R(\lambda_0)$, its width $\Delta\lambda_1$ defining v_1. More generally it indicates that the wind contains no material of $v < v_1$. (The well known case of a purely rectangular profile is a special case of this in which the entire wind has the same finite speed.)

Outside any central flat region Eqs. (7), (8) become

$$L_\lambda(\Delta\lambda) = \frac{2\pi c}{\lambda_0} \int_{c\Delta\lambda/\lambda_0}^{v_\infty} \frac{r^2(v) j(r(v))\mathrm{d}v}{v \mathrm{d}v/\mathrm{d}r} \tag{9}$$

which has inverse solution

$$\frac{r^2(v) j(r(v))}{v \mathrm{d}v/\mathrm{d}r} = -\frac{\lambda_0^2}{2\pi c^2} \left(\frac{\mathrm{d}L_\lambda}{\mathrm{d}\lambda}\right)_{\Delta\lambda = v\lambda_0/c} \tag{10}$$

allowing the function $v(r)$ on the left hand side to be derived from the data function on the right.

In order to obtain $v(r)$, it is necessary to know $j(r)$ for the line concerned. In our optically thin case this will depend on the wind density $n(r)$ and temperature $T(r)$ and directly on r if the line emission is partly governed by stellar illumination diluted by $(R/r)^2$.

For a steady state wind, $n(r)$ is uniquely related to $v(r)$ by continuity, viz

$$n(r) = \frac{\dot{M}}{4\pi r^2 v(r) \bar{m}} \tag{11}$$

where $\dot{M}$ is the stellar mass loss rate and $\bar{m}$ is the mean mass per electron present, if $n(r)$ is the electron density (i.e. $n\bar{m} = \rho$, the mass density).

The variation of $T(r)$ is more complex, being governed by energy transport considerations. In order for Eq. (10) to be used to yield $v(r)$, it is necessary to parametrise the $T(r)$ variation or to express it in terms of r, $n(r)$ and the stellar luminosity so that the left side of Eq. (10) depends only on $v(r)$ and r. Here we consider the simplest possible case where T is approximately a constant, T_0. For definiteness we examine the solution for a recombination line with

$$j(r) = n^2(r) f_0(T_0) \tag{12}$$

where $f_0(T_0)$ is the relevant atomic recombination coefficient $\times hc/\lambda_0$.

Then, for a recombination line at constant T_0, Eq. (10) becomes, using Eq. (11),

$$\left(\frac{\dot{M}}{4\pi r^2 \bar{m} v(r)}\right)^2 f_0 \frac{r^2}{v \mathrm{d}v/\mathrm{d}r} = -\frac{\lambda_0^2}{2\pi c^2} \left(\frac{\mathrm{d}L_\lambda}{\mathrm{d}\lambda}\right)_{\Delta\lambda = v\lambda_0/c} \tag{13}$$

which can be rewritten as

$$\frac{\mathrm{d}v^4}{\mathrm{d}(1/r)} = \frac{f_0}{2\pi} \left(\frac{\dot{M}c}{\bar{m}\lambda_0}\right)^2 \frac{1}{\left[\mathrm{d}L_\lambda/\mathrm{d}\lambda\right]_{\Delta\lambda = v\lambda_0/c}} \ . \tag{14}$$

This is a differential equation for v^4 as a function of $1/r$ which can be solved numerically to yield $r(v)$ (and hence $v(r)$ for this monotonic case) for a data set on L_λ and specified $\dot{M}/\bar{m}$, viz

$$r(v) = \frac{f_0}{2\pi} \left(\frac{\dot{M}c}{\bar{m}\lambda_0}\right)^2 \Bigg/ \int_v^{v_\infty} \left[-\frac{\mathrm{d}L_\lambda}{\mathrm{d}\lambda}\right]_{\frac{\Delta\lambda}{\lambda_0} = \frac{v}{c}} \mathrm{d}v^4 \tag{15}$$

where L_λ is related to the observed line flux spectrum F_λ(W m^{-2} per unit λ) at the earth, distance D by

$$L_\lambda = 4\pi D^2 F_\lambda \ . \tag{16}$$

So

$$r(v) = \frac{f_0}{8\pi^2}\left(\frac{\dot{M}}{D}\right)^2\left(\frac{c}{\bar{m}\lambda_0}\right)^2 \Big/ \int_v^{v_\infty}\left[-\frac{\mathrm{d}F_\lambda}{\mathrm{d}\lambda}\right]_{\Delta\lambda=\lambda_0\frac{v}{c}} \mathrm{d}v^4. \tag{17}$$

Note that we deal solely with the line flux, assuming the continuum flux to have been subtracted. We note also that the solution for $r(v)$ scales as the factor $(\dot{M}/D)^2$ since two stars of different $\dot{M}$ values will give exactly the same recombination line profile, $F_\lambda(\Delta\lambda)$, if the star of higher $\dot{M}$ is at a proportionately higher distance D. Alternatively, stars of the same D and the same observed profile $F_\lambda(\Delta\lambda)$ will yield similar solutions for $r(v)$ but with the r scale modified proportionally to $\dot{M}^2$ because the emissivity per unit r scales as $n^2(r) \propto \dot{M}^2$ for a given $v(r)$. In other words, a given line flux $F_\lambda(\Delta\lambda)$ results from a smaller volume in a denser wind. The form of dependence of the equation on $(\dot{M}, D)$ will differ for different types of lines (i.e. non-recombination) – a fact which may help unravel the values of $\dot{M}$ and D when dealing with real data, as we discuss in a subsequent paper (Brown et al. in preparation). For the present we assume $\dot{M}$, D to have known values and develop our inversion method for suitable dimensionless variables (Sect. 4).

We also note that the solution Eq. (17) involves differentiation of the data and consequent amplification of data noise. This relates directly to the point made earlier concerning uniqueness of the solution or, equivalently, of the information on $v(r)$ contained in the noisy line profile. However, solutions involving such simple data differentiation are only moderately ill-posed compared to many inverse problems (Craig and Brown 1986). Furthermore, $v(r)$ in Eq. (17) is derived from $\mathrm{d}L_\lambda$ by *integration* of differential Eq. (14), the integration process smoothing much of the instability – see Sect. 5.

4. Solution procedure

For numerical and evaluation purposes it is best to express Eqs. (14) and (17) in dimensionless form for which we use the variables

$$\begin{aligned} y &= \frac{R}{r}, & w(y) &= \frac{v(r)}{v_\infty} \\ t &= \frac{\Delta\lambda}{\Delta\lambda_{\max}}, & \phi(t) &= \frac{8\pi^2 D^2 \bar{m}^2 \lambda_0 R v_\infty^3}{f_0 \dot{M}^2 c} F_\lambda \\ f(t) &= \frac{\mathrm{d}\phi}{\mathrm{d}t} \end{aligned} \tag{18}$$

where $\Delta\lambda_{\max} = \lambda_0 v_\infty/c$ is the extreme of the the line profile spread (after removal of any electron scattering wings) and R is any convenient scale distance of the order of the estimated stellar photospheric radius for the line wavelength λ_0 considered.

To proceed we need to assume values for the constants appearing in front of F_λ in Eq. (18). That is, we need to adopt values for $\dot{M}$, D and R; f_0 and $\bar{m}$ are assumed known.

In terms of the above variables, $w(0) = 1$ by definition of v_∞. The inverse problem and its solution become

$$\phi(t) = \frac{1}{4}\int_0^{y(w=t)} \frac{\mathrm{d}y}{w^3} = \int_1^t \frac{\mathrm{d}w}{\mathrm{d}w^4/\mathrm{d}y} \tag{19}$$

and

$$\frac{\mathrm{d}w^4}{\mathrm{d}y} = \frac{1}{[f(t)]_{t=w}} \Rightarrow y(w) = \int_{w^4}^1 [-f(t)]_{t=w}\,\mathrm{d}w^4 \ . \tag{20}$$

The data analysis procedure is to find $\Delta\lambda_{\max}$ from the line profile limit ($F_\lambda \to 0$ after continuum subtraction), evaluate $f(t)$ from $\mathrm{d}F_\lambda/\mathrm{d}\lambda$ at a grid of points $t = \Delta\lambda/\Delta\lambda_{\max}$ for a specified value of $\dot{M}/D$, then march 'inward' in r (outward in y) along the profile grid $f(t)$ from $w = 1$ ($v = v_\infty$) to value w evaluating $y = R/r$ at each $w = v/v_\infty$ from Eq. (20) for an assumed R value.

Before showing the results of this procedure for various trial functions, $v(r)$, and corresponding simulated data $F_\lambda(\Delta\lambda)$, we observe the following points:

1. We have assumed $v(r)$ monotonic and, for definitiveness, $v'(r) > 0$. For an optically thin flow it is not possible to discriminate, from F_λ, between a wind outflow ($v' > 0$) and an accretion inflow ($v' < 0$) since the front and rear hemispheres are interchangeable (when flow occultation by the finite stellar disk is neglected as we have done.)
2. Our inversion equations have dealt solely with Eq. (8) in that part of the line profile outside any central flat portion of width $\Delta\lambda_1 = (v_1/c)\lambda_0$ corresponding to a finite $v(R) = v_1$ at the stellar 'photosphere' of radius R_0 at this wavelength, λ_1. If the above solution procedure is followed from $t = 1$ ($w = 1$, $v = v_\infty$) to the profile 'shoulder' point $t_1 = \Delta\lambda_1/\Delta\lambda_{\max} = v_1/v_\infty$ and there we find $y = R/r = y_1$ then we can find the value $r_1 = R/y_1$ at which $v = v_1$. Then r_1 is the value of the photospheric radius at λ_0 in units of R for the adopted values of $(\dot{M}/D)^2$ which arises in Eqs. (17) and (18), and its absolute value R_0 scales as this factor. If we know R_0, we can find the value of $\dot{M}/D$, or if we know $\dot{M}/D$ we can find R_0.
3. If the wind has $v'(r) \geq 0$ so that $v(r)$ never decreases with increasing r but in some region r_1, r_2 ($> R_0$) has a constant speed v_1, the equations have to be considered slightly differently. The previous solution analysis applies as we march inward along the monotonic profile to the point $\Delta\lambda_1$ corresponding to wind speed v_1 at distance r_2 where $v \to v_1$. At this point v becomes constant ($\mathrm{d}v/\mathrm{d}r = 0$) over a finite range of r, and we see from Eq. (7) that we must revert to form (6) of the original equation which shows that, at this $\Delta\lambda_1$, the profile $F_\lambda(\Delta\lambda)$ will become 'vertical', i.e. there will be a finite step upward in F_λ at $\Delta\lambda = \Delta\lambda_1$, the 'height' of which will be (using $F_\lambda = L_\lambda/4\pi D^2$ and $j(r) = (\dot{M}/4\pi r^2 \bar{m} v(r))^2 f_0$)

$$\begin{aligned} \Delta F_\lambda &= \frac{c}{32\pi^2\bar{m}^2\lambda_0}\frac{\dot{M}^2}{v_1^2 D^2}\int_{r_1}^{r_2}\frac{\mathrm{d}r}{r^2} \\ &= \frac{c}{32\pi^2\bar{m}^2\lambda_0}\frac{\dot{M}^2}{v_1^2 D^2}\left(\frac{1}{r_1}-\frac{1}{r_2}\right) \ . \end{aligned} \tag{21}$$

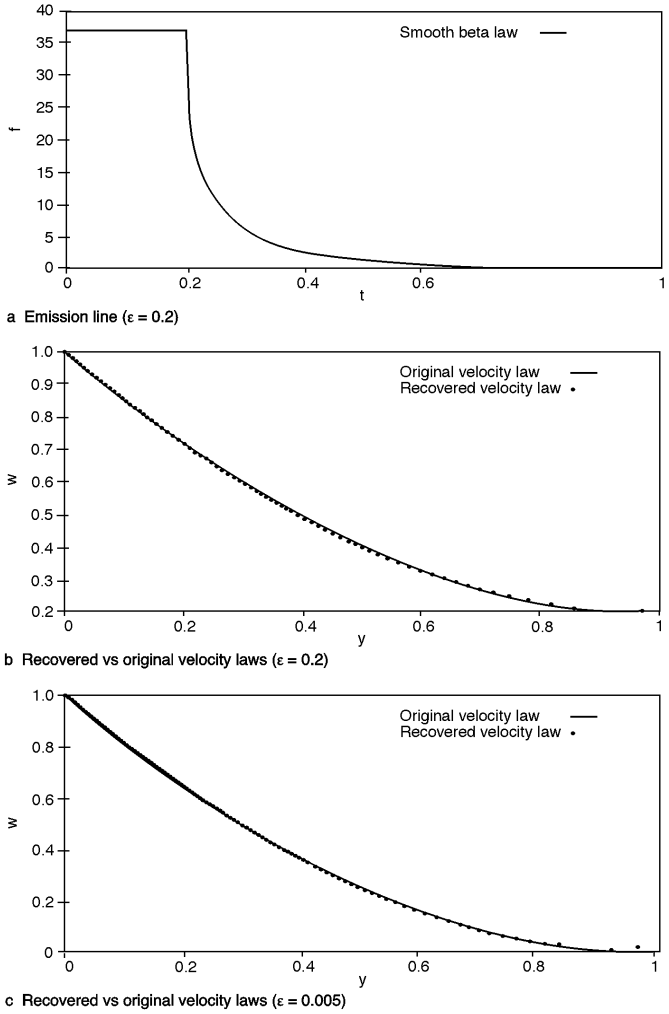

Fig. 3. Smooth β law with non-zero initial velocity

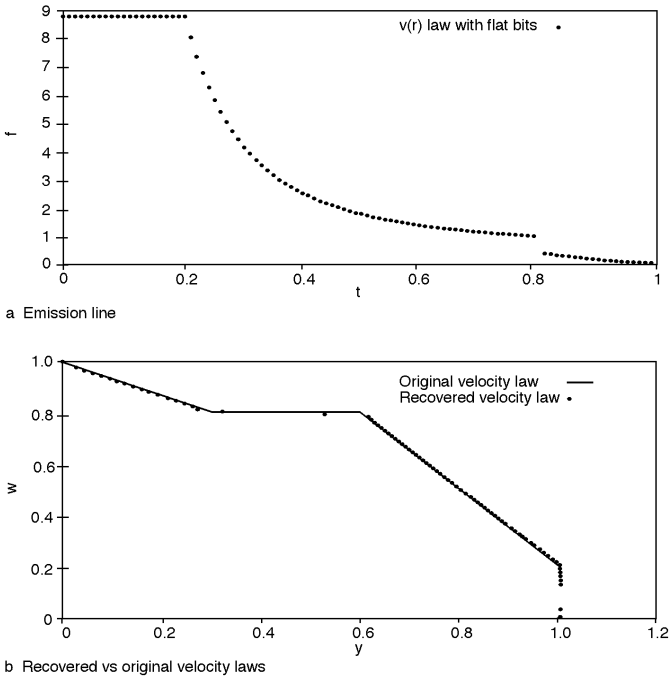

Fig. 4. Velocity law with flat portion

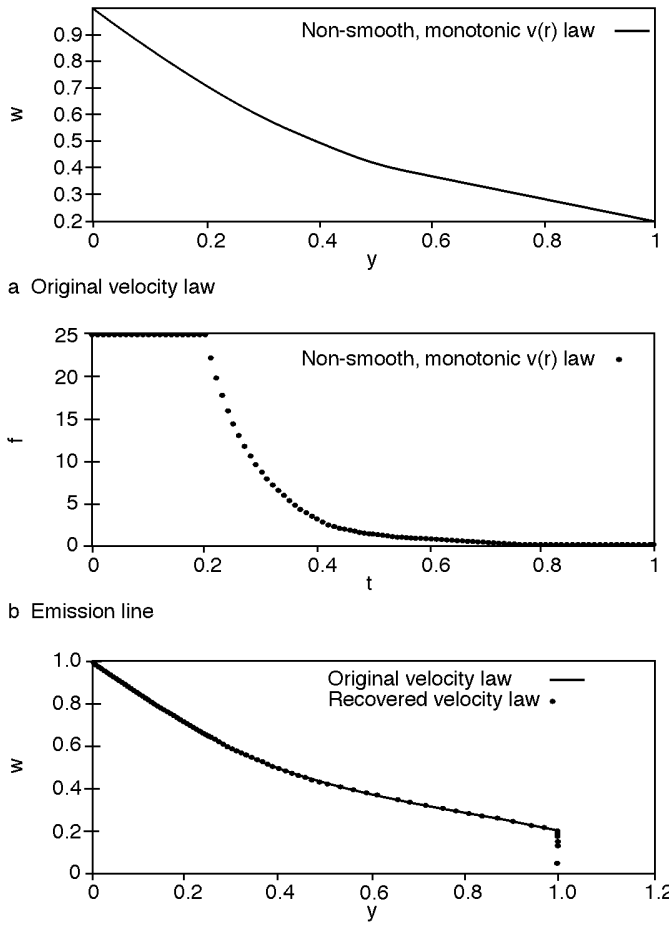

Fig. 5. Non-smooth, monotonic $v(r)$ laws

Thus there is a finite change in $(1/r)$, as there is in $F_\lambda(\Delta\lambda)$, for an infinitesimal change in $\Delta\lambda$. Since r_2 is known from integration inward of the monotonic line profile up to this point, measurement of ΔF_λ yields the value of r_1 from Eq. (21) and the previous procedure resumes inward from $r = r_1$ along the monotonic line profile at $\Delta\lambda \leq \Delta\lambda_1$ until the next such profile step is reached (and treated similarly), the process being continued until either $\Delta\lambda = 0$ is reached or a central profile plateau is reached in the range $|\Delta\lambda| \leq \Delta\lambda_1$ corresponding to a finite photospheric speed v_1 as discussed in point (2) above. In fact the numerical inversion procedure we used generates this finite step in r automatically.

5. Results for parametric $v(r)$ and simulated $F_\lambda(\Delta\lambda)$

We created emission lines for various $v(r)$ using Eq. (9) and then inverted them using the technique described above. By examining the results of the inversion, i.e. the recovered velocity law, and then comparing this with the original velocity law, we confirmed the validity of our code. Throughout this section

we use the dimensionless variables defined in Eq. (18) when plotting results.

Smooth β law

A common form of velocity law used in the literature is the β law, $w = (1-y)^\beta$ or

$$v(r) = v_\infty \left(1 - \frac{R}{r}\right)^\beta \quad . \tag{22}$$

Our basic model cannot cope directly with this type of law except at $r > R$ since, as $r \to R$, $v \to 0$ and $n \to \infty$ (Eq. 11) so that $F_\lambda(\Delta\lambda) \to \infty$ at $\Delta\lambda \to 0$ (Eq. 13). In reality the fact that $n \to \infty$ where $v \to 0$ implies infinite optical depth and we could truncate our inward marching solution at a value of $r/R_0 > 1$ where the optical depth exceeds unity. In practise it proved possible to continue our solutions close to $r = R_0$, i.e. to $v << v_\infty$.

Smooth β law with finite speed at $r = R$

The problem described above does not arise for modified β laws of the form

$$v(r) = v_\infty \left[\varepsilon + (1-\varepsilon)\left(1 - \frac{R}{r}\right)^\beta\right] \tag{23}$$

since $v(R) = \varepsilon v_\infty \neq 0$ (as long as $\varepsilon \neq 0$) and so $n \not\to \infty$. The emission line created using such a law (with $\beta = 2$ and $\varepsilon = 0.2$) is shown in Fig. 3a, and in Fig. 3b we show the original and recovered velocity laws. In Fig. 3a we can clearly see the flat top of the profile which is indicative of a non-zero velocity at $r = R$ as discussed above. In Fig. 3b we can see that the model has recovered the original velocity law.

We also carried out the procedure with $\varepsilon = 0.005$. For a value of ε as small as this, we are essentially modelling the type of law described above, as $\varepsilon = 0.005$ corresponds to an initial wind speed of $\sim 5\text{km s}^{-1}$, which is below the ion thermal speed. The results of this inversion are shown in Fig. 3c.

$v(r)$ laws with flat portions

We now turn our attention to laws of the form

$$v(r) = \begin{cases} v(r) & R \le r \le r_1 \\ v_1 & r_1 \le r \le r_2 \\ v(r) & r \ge r_2 \end{cases} \tag{24}$$

i.e. velocity laws which are not monotonic but instead have a constant velocity in a specific region $[r_1, r_2]$. The emission line in Fig. 4a was created using the specific $v(r)$ law

$$v(r) = \begin{cases} \varepsilon v_\infty + \frac{(v_1 - \varepsilon v_\infty)(r-R)}{(r_1 - R)} & R \le r \le r_1 \\ v_1 & r_1 \le r \le r_2 \\ v_1 - \frac{(v_\infty - v_1)(r_2 - r)}{r} & r_2 \le r \le \infty \end{cases} \tag{25}$$

with $\varepsilon = 0.2$, $r_1 = 5R/3$, $r_2 = 10R/3$ and $v_1 = 0.8 v_\infty$. This emission line was then inverted using the *same* procedure as for

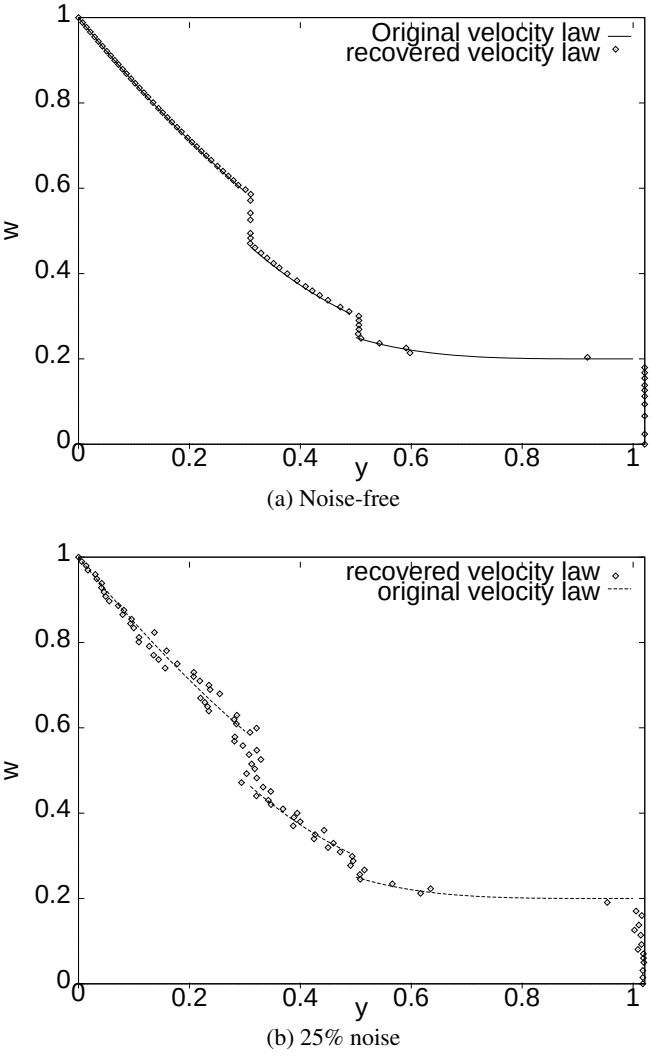

(a) Noise-free

(b) 25% noise

Fig. 6. Recovered *vs* original velocity law: Discontinuous, non-smooth, monotonic velocity law

emission lines created with wholly monotonic $v(r)$ laws, and we see that the procedure detailed in point (3) above is already implicit in the code used. The routine again finds and recovers the flat portion of the velocity profile (Fig. 4b) though, by the nature of the problem, the code only picks out two discrete points in the flat portion.

Non-smooth but monotonic $v(r)$

Here we use a velocity law of the form

$$v(r) = \begin{cases} v_\infty \left[\varepsilon + \frac{(R/r - 1)}{(R/r_1 - 1)}\left(w_3 + w_2 - \varepsilon\right)\right] & R \le r \le r_1 \\ v_\infty \Big[\varepsilon + (1-\varepsilon)\left(1 - \frac{R}{r}\right)^{\beta_2} & \\ \qquad + w_1 - w_2\Big] & r_1 \le r \le r_2 \\ v_\infty \left[\varepsilon + (1-\varepsilon)\left(1 - \frac{R}{r}\right)^{\beta_1}\right] & r_2 \le r < \infty \end{cases} \tag{26}$$

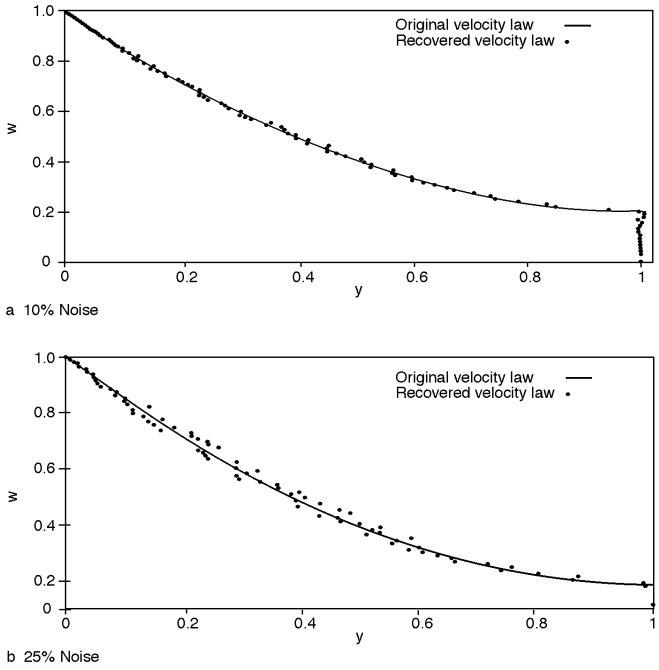

Fig. 7. Recovered *vs* original velocity law: smooth β law

where

$$w_1 = \varepsilon + (1-\varepsilon)\left(1 - R/r_2\right)^{\beta_1}$$
$$w_2 = \varepsilon + (1-\varepsilon)\left(1 - R/r_2\right)^{\beta_2}$$
$$w_3 = \varepsilon + (1-\varepsilon)\left(1 - R/r_1\right)^{\beta_2} \ .$$

To model this law we took the following values for the variables: $\beta_1 = 2$, $\beta_2 = 3$, $r_1 = 2R$, $r_2 = 10R/3$, and $\varepsilon = 0.2$. This velocity law is shown in Fig. 5a, the resulting emission line in Fig. 5b and the results of the inversion in Fig. 5c. As before, despite the non-smoothness of the velocity law, the inversion routine recovers it well, which is unusual for an inverse problem, unless regularisation/smoothing is applied. This is because here the solution $v(r)$ is an integral of the inverted data, as already noted.

This particular velocity law was continuous. We also investigated the case where the law was non-smooth, monotonic and discontinuous. This law was of the form

$$v(r) = \begin{cases} v_\infty \left[\varepsilon + (1-\varepsilon)\left(1 - \frac{R}{r}\right)^{\beta_3}\right] & R \le r \le r_1 \\ v_\infty \left[\varepsilon + (1-\varepsilon)\left(1 - \frac{R}{r}\right)^{\beta_2}\right] & r_1 < r < r_2 \\ v_\infty \left[\varepsilon + (1-\varepsilon)\left(1 - \frac{R}{r}\right)^{\beta_1}\right] & r_2 \le r < \infty \end{cases} \quad (27)$$

with $\varepsilon = 0.2$, $\beta_1 = 2$, $\beta_2 = 3$ and $\beta_3 = 4$. The results of this inversion are shown in Fig. 6a.

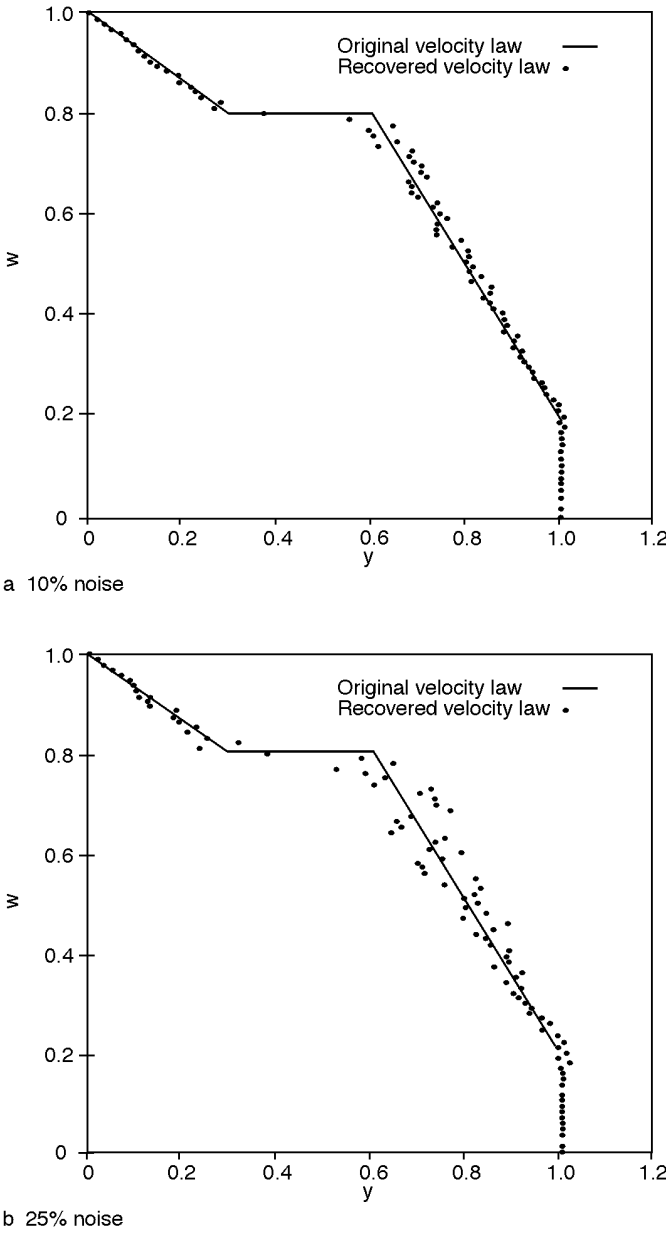

Fig. 8. Recovered *vs* original velocity law: $v(r)$ law with flat portion

The effect on $v(r)$ of noise on F_λ

We reconsidered the $v(r)$ laws detailed above but with random noise added to data points $F_\lambda(\Delta\lambda)$. First we used the smooth β law with a finite speed at $r = R$, leaving all parameters unchanged but adding in first 10% and then 25% noise on F_λ. The results of the inversion are shown in Fig. 7. As can be seen from these plots, even with noise added to the emission line, the inversion routine can still recover the velocity law of the wind remarkably well, for the reasons given at the end of Sect. 3.

The effects of noise on recovery of a velocity law with a 'flat' portion are shown in Fig. 8 and for a discontinuous one in Fig. 6b. Only in the case of noise as large as 25% does some

loss of recovered structure occur, even in the case of sharp discontinuities as shown in Fig. 6.

6. Discussion

We have demonstrated that, under various idealisations, it is possible to recover, without prior parametric assumptions, the velocity profile $v(r)$ of a stellar wind from the profile of a wind emission line, by solution of an integral equation, the inversion being quite well posed in the presence of noise. The main idealisations made are: low wind optical depths (absorption and scattering); neglect of wind absorption of the stellar disk continuum in the blue wing; neglect of stellar occultation of wind emission in the red wing. The influence of these effects on the accuracy of the method will be analysed in subsequent papers, as will the benefits of using several emission lines together.

Acknowledgements. This work was supported by UK PPARC Rolling, STARLINK and Visitor grants and in part by NSF Grant AST-9417186 to the University of Wisconsin. Brown wishes to thank A.F.J. Moffat and the Montreal Group for many helpful discussions.

References

Brown, J.C., Richardson, L.L., Antokhin, I., Robert, C., Moffat, A.F.J, St-Louis, N. 1995, A&A, 295, 725
Cannon, C.J. 1974, A&A, 34, 387
Craig, I.J.D., Brown, J.C. 1986, Inverse problems in Astronomy; a guide to inversion strategies for remotely sensed data, Bristol and Boston
Hamman, W.R. 1981, A&A, 93, 353
Lamers, H.J.G.L.M., Cerruti-Sola, M., Perinotto, M. 1987, ApJ, 314, 726
Lamers, H.J.G.L.M., Cassinelli, J.P. 1997, Introduction to Stellar Winds, Cambridge Press: Cambridge
Moffat, A.F.J., Robert, C. 1992, ASPC, 22, 203
Robert, C. 1994, Ap&SS, 221

This article was processed by the author using Springer-Verlag LaTeX A&A style file *L-AA* version 3.